Published by IOP Publishing for Sissa Medialab

Received: *February 12, 2020*
Accepted: *February 28, 2020*
Published: *April 1, 2020*

Radiation detection materials for quality assurance and dose distribution assessment of small fields of high-energy X-rays

Sung Jin Noh,[a,b] **HyoJin Kim,**[a] **Hyun Kim,**[a] **Jeung kee Kim,**[a] **Chi-Woong Mun**[b] **and Yeong-Rok Kang**[a,1]

[a] *Research Center, Dongnam Institute of Radiological & Medical Sciences, Busan, Republic of Korea*
[b] *Biomedical Engineering, Inje University, Gimhae, Gyeongnam, Republic of Korea*

E-mail: yeongrok@dirams.re.kr

Abstract: This paper present a system for an integrated radiotherapy quality assurance (QA) protocol that maintains dose measurement accuracy through a dosimeter capable of accurate small-field dosimetry. The beam pulse data of a linear accelerator (LINAC) was obtained, and its conformity with the photoconductor material detection signal was evaluated. To determine the radiation detection material for dose measurement, unit-cell-type specimens were fabricated through sedimentation from four candidate materials (lead II iodide, PbI_2; lead II oxide, PbO; mercury II iodide, HgI_2; and a mixture of HgI_2 and titanium dioxide, TiO_2). Based on evaluations of dark current, output current, rising time (10%–90%), falling time, and response delay, the mixed $TiO_2$and HgI_2material exhibited the best characteristics. Accordingly, we fabricated 3×3 and 6×6 multi-pixel arrays capable of small-field dosimetry. The 3×3 multi-pixel array had a pixel size of 3 cm × 3 cm; the thickness of the detection material was approximately 400 μm. LabVIEW was used to design the arrays. Analog signals generated in each pixel were converted to digital signals through an analog-to-digital converter, displayed in a waveform, and stored. The 6×6 multi-pixel array had pixels of diameter of 1 mm and pixel pitch of 1 mm; thickness of the detection material was approximately 485 μm. A LINAC was used to evaluate the arrays according to the detection characteristics and dose changes at acceleration voltages of 4, 6, 10, and 15 MV. Excellent reproducibility, linearity, and accuracy were confirmed by comparing the dose detector and response characteristics to actual cases. This study verifies the applicability of photoconductor-based solid-state detectors, which can replace existing dosimeters for small-field QA, and proposes a new protocol to simplify complex and difficult radiotherapy QA procedures, thereby increasing user convenience.

Keywords: Materials for solid-state detectors; Solid state detectors; X-ray detectors

[1] Corresponding author.

https://doi.org/10.1088/1748-0221/15/04/P04001

2020 JINST 15 P04001

Contents

2020 JINST 15 P04001

1 Introduction

Radiotherapy is one of the three major treatments for cancer, along with surgery and chemotherapy. Surgical treatment, traditionally a radical wide resection, has been the most important component of cancer treatment. However, integration of the three treatment methodologies has become increasingly common due to advances in knowledge and experience in pathophysiology, radiation biology, and radiophysics. Thus, the role of radiotherapy has concurrently increased over time, particularly as radiotherapy can effectively suppress tumors without tissue and organ loss. For successful radiotherapy, sufficient radiation is applied to a tumor site to suppress tumor growth. Simultaneously, the radiation dose to the surrounding normal tissues is limited to minimize the risk of acute side effects and chronic complications. For this purpose, it is vital to establish a treatment plan with accurate and precise dose measurements and to reduce inconsistencies in treatments [1, 2].

Radiosurgery is a sophisticated treatment method in which a high dose of radiation (10–30 Gy per round) is delivered to the treatment site using a linear accelerator (LINAC). Recently, LINACs with multi-leaf collimators (MLCs) have emerged and LINACs are finding increased applications in

radiosurgery. In this treatment method, high doses of radiation are concentrated in small fields; thus, overexposing normal tissue to the radiation can lead to numerous side effects, including fatality. Therefore, systematic and accurate quality assurance (QA) is critical [3–8].

Accurate dose distribution and dosimetry are both essential to effective QA. Accordingly, an appropriate detector with high spatial resolution, accurate dose mapping, and accurate dosimetry of the penumbra is needed to accurately measure small-field dose characteristics. Furthermore, the detector should be able to minimize the effect of lateral electronic disequilibrium, which may indicate errors in the small-field dosimetry. Generally, a thermoluminescence dosimeter, diode detector, ionization chamber, diamond detector, film, or other similar device, is used to measure small-field dose characteristics. Several previous studies have discussed the advantages and disadvantages of each type of detector for small-field dosimetry [9–13]. However, additional information regarding the delivery of radiation in radiosurgery is needed to guide the development of novel devices and to ensure patient safety. To this end, this study provides basic data for the development of equipment and dose distributions to mitigate the disadvantages of QA devices with regards to their current high-energy characteristics and small fields.

2 Materials and methods

2.1 Photoconductor selection and sensor fabrication

In this study, a photoconductor detector was fabricated for use as a dosimeter for radiation in high-energy bands irradiated by LINACs. The LINACs accelerate electrons in a linear accelerating tube using high-frequency electromagnetic waves, thus generating high-energy radiation. As with electron beams, it is difficult to represent the generated photon beams through a single variable (e.g. maximum energy, average energy). In addition, the high-energy radiation that is produced mainly causes Compton scattering due to its interaction with the detection material. Thus, unlike the photoelectric effect, which is affected by the atomic number, materials with higher electron densities exhibit higher signal generation efficiencies [14]. Previously, silicon was used as the primary photoconductor for solid-state-type detectors. However, in the present study, four unit-cell-type specimens were fabricated from four candidate materials (lead II iodide, PbI_2; lead II oxide, PbO; mercury II iodide, HgI_2; and a mixture of HgI_2 and titanium dioxide, TiO_2) whose performances were confirmed by previous literature [15–20]. Materials with strong signal generation efficiency were selected through a characterization of the unit-cell-type specimens and were subsequently used to fabricate 3×3 and 6×6 multi-pixel arrays for small-field dosimetry.

2.1.1 Fabrication of unit-cell-type therapeutic high-energy radiation conversion materials

This study evaluated the reactivity of a high-energy band irradiated by the LINAC to verify the signal generation efficiency of the specimens fabricated from the four materials. The raw materials used in the fabrication of the specimens consisted of 99.999% mercury (II) iodide, lead (II) oxide, and 99.99% lead (II) iodide produced by the Kojundo chemical laboratory, and 99.5% titanium dioxide produced by CERAC. Deposition methods for photoconductor materials include physical vapor deposition, chemical vapor deposition, and the particle-in-binder (PIB) method, among others; this study used the PIB method. Poly-vinyl-butyral was added to a solution of diethylene glycol

2020 JINST 15 P04001

mono-butyl ether acetate (DGMA) and the dispersant diethylene glycol mono-ethyl ether (DGME) to prepare a binder solution. For the unit-cell-type specimens, PbI_2, PbO, HgI_2, and the HgI_2 and TiO_2 mixture were deposited through sedimentation — a PIB method — on the glass substrate on which indium thin oxide (ITO) was formed. ITO was then formed as the top electrode using a DC magnetron sputtering device [21]. The active area of the prepared specimens was 1 cm × 1 cm, and the thickness of the photoconductor layer was approximately 400 µm. Figure 1 shows a diagram of the fabrication process of the specimens.

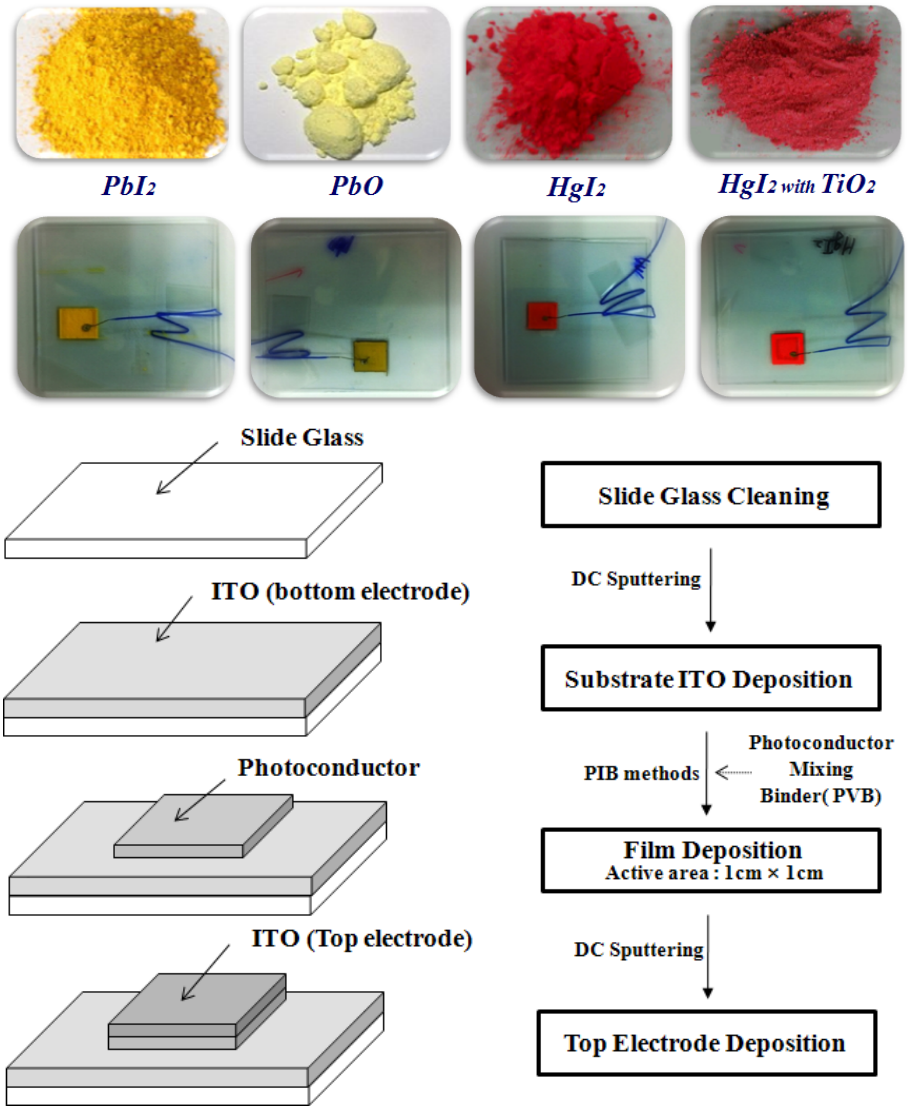

Figure 1. (a) Fabrication of 1 cm × 1 cm unit-cell specimens using photoconductor materials, and (b) process schematic of specimen fabrication. ITO = indium thin oxide; PIB = particle-in-binder; PVB = poly-vinyl-butyral.

2020 JINST 15 P04001

2.1.2 Fabrication of a 3 × 3 multi-pixel array sensor

After the characterization of the unit-cell-type specimens, the HgI_2 + TiO_2 mixture — which has excellent radiation response characteristics — was deposited by the PIB method. Gold was then deposited as the upper electrode through the evaporation deposition system. Figure 2 shows the fabricated sensor which is comprised of nine channels arranged in a 3 × 3 array. Each pixel has an active area of 3 cm × 3 cm, and the thickness is approximately 400 µm. A test jig was constructed to detect the signal of each pixel, and a separate form was prepared to connect the readout to the pixels.

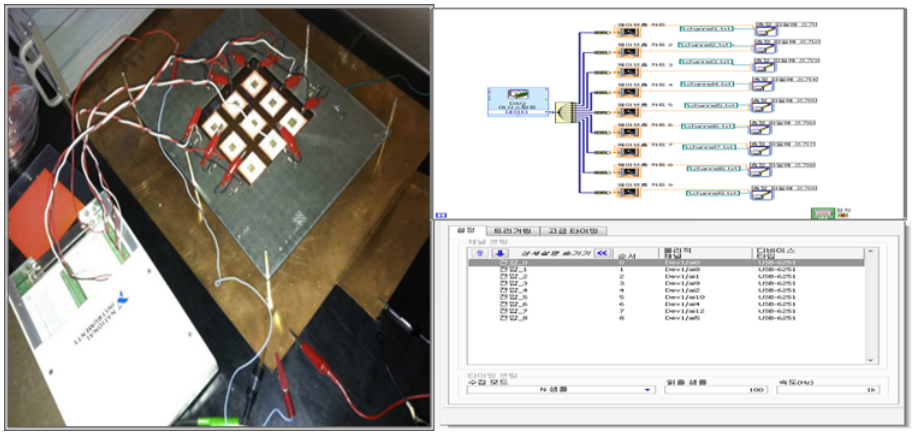

Figure 2. Fabricated 3 × 3 multi-pixel array sensor hardware and software.

To detect the multi-pixel signals, a data acquisition system (DAQ) environment was constructed using a tool provided in the program LabVIEW. Then, the radiation dose of high-energy bands was verified, with regards to the reproducibility and linearity of the detection signals. Finally, the beam pulse and sensor data signals were compared to validate the DAQ.

2.1.3 Fabrication of a 6 × 6 multi-pixel array sensor

This study verified the development of a multi-pixel sensor, which directly verifies the small-field high-energy radiation dose. Accordingly, considering the size of the MLC mounted on a general LINAC (figure 3), 36 holes of 1 mm diameter each were drilled and plated with gold on the PCB substrate; thus, each of them formed an electrode. These electrodes served each pixel in the top electrode of the sensor when the selected photoconductor material was deposited for future sensor fabrication. Thus, it was fabricated using gold, which does not chemically react with photoconductor materials, and the PCB substrate was used considering the transmissivity of the therapeutic high energy radiation. The photoconductor material selected for the characterization of the unit-cell-type radiation detection specimen, the HgI_2 and TiO_2 mixture, was used to fabricate the array with a pixel size of 1 × 1 mm^2 and a pixel pitch of 1 mm on the PCB substrate. The array had a thickness of approximately 485 µm and a total area of 2 × 2 cm^2. To collect the signals obtained from the 36 pixels during irradiation, the analog signals were processed as digital signals using the analog-to-digital converter, ADC-CD40151BC, after which a separate tool for the collection of signal processing data, MCU-C8051F020, was used.

2020 JINST 15 P04001

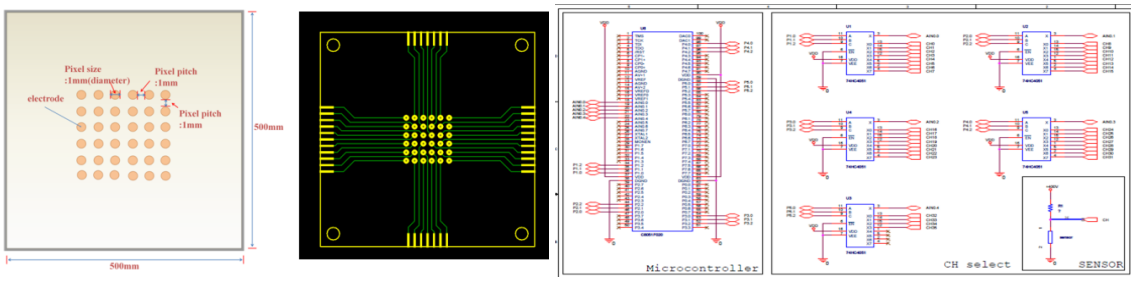

Figure 3. 6 × 6 multi-pixel array sensor PCB design, structure, and hardware black diagram.

2.2 Dosimetry and evaluation method

In this study, a unit-cell-type specimen was fabricated to verify the radiation response characteristics of the high-energy bands of the photoconductor materials. A multi-pixel array was also fabricated to verify the radiation dose, which includes the reproducibility and linearity of small-field radiation in the high-energy bands. A Synergy LINAC (Elekta) and Clinac iX LINAC (Varian) were used to validate the fabricated specimen and sensor. Acceleration voltages of 4, 6, 10, and 15 MV were used in the experiments to produce high-energy X-rays in the therapeutic radiation range. Accounting for sensor size, the irradiation size was fixed at $10 \times 10\,cm^2$ for the 3 × 3 multi-pixel array sensor and $2 \times 2\,cm^2$ for the 6 × 6 multi-pixel array sensor.

2.2.1 LINAC beam pulse detection

A LINAC uses high-frequency electromagnetic waves to accelerate charged particles, such as electrons, to a high energy through a linear tube. In particular, the LINAC collides accelerated electrons with the transmission target to generate X-rays. Moreover, as the acceleration tube in the high-energy LINACs is very long, it is placed horizontally or horizontally at an angle. The electrons therefore bend at an appropriate angle (usually approximately 90° or 270°) between the accelerator tube and the target, and subsequently collide with the target. As shown in figure 4, the beam pulse data of the LINAC, which generates flux, is designed to collect the signals of the output generated when the electrons collide with the target. The signals were confirmed using an oscilloscope (LeCroy, 62 Xi, U.S.A.).

2.2.2 Evaluation of photoconductor sensor characteristics for a beam pulse

The goal of this study was to develop a QA device to measure the dose of high-energy radiation with excellent efficiency in small fields. Therefore, evaluation of the electrical characteristics of the sensor is crucial. Figure 5 is a schematic diagram of the setup used to confirm the electrical characteristics of the unit-cell-type specimen and the multi-pixel array sensor. After fixing the source-to-surface distance (SSD) at 100 cm, we confirmed the radiation response characteristics according to the changes in the radiation energy and energy intensity. For this purpose, an electrometer (Keithley, 6517A, U.S.A.) and an oscilloscope (LeCroy, 62 Xi, U.S.A.) were used. A driving voltage of 1 V/μm was applied, and the output signal of the charge collected through the electrometer was confirmed through the oscilloscope; after this, the charge signal was stored as digital data.

2020 JINST 15 P04001

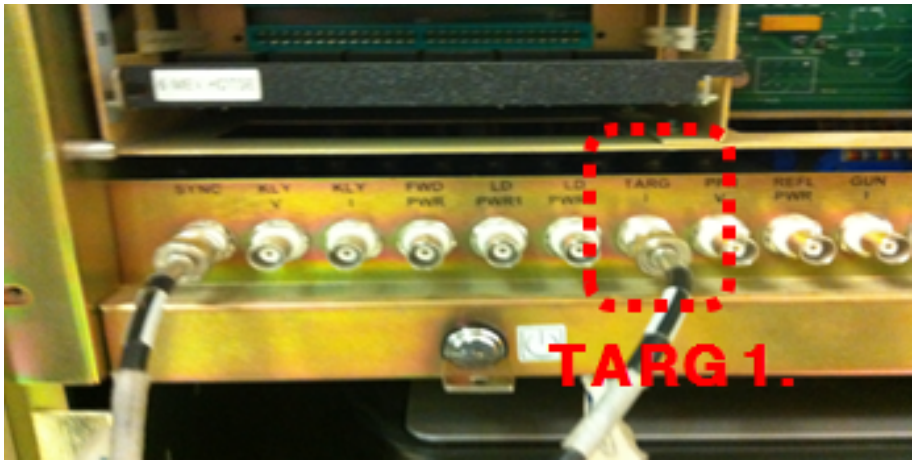

Figure 4. Beam pulse data collection setup.

For the unit-cell-type specimens, the detection characteristics were analyzed through experiments on dark current, output current, rising time, falling time, and response delay to select photoconductor materials with excellent detection characteristics for high-energy radiation. We also verified the conformity of the detection signal and the beam pulse signal of the LINAC. This study additionally evaluated the reproducibility, accuracy, and linearity of the multi-pixel array sensor fabricated with the photoconductor materials selected by characteristic analysis.

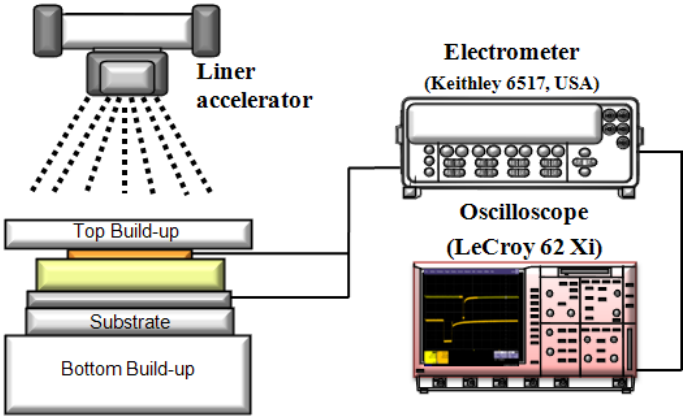

Figure 5. Schematic of signal collection setup for dose detection.

2.2.3 Dose evaluation by monitor unit

To evaluate the unit cell, an assessment of the detector characteristics was performed to select superior photoconductor materials for radiation detection. Accordingly, the following evaluations were performed:

(1) Conformity — the detection specimen signals were verified by comparison to the LINAC beam pulse as a benchmark

2020 JINST 15 P04001

(2) Reproducibility — high-energy radiation was delivered 10 times at a fixed dose rate of 400 monitor units (MU)/min at 100 MU and acceleration voltages of 6 MV and 15 MV. The delivered dose of radiation was confirmed.

(3) Linearity — MU was increased linearly to irradiate at a high energy, during which the dose generated in the unit-cell-type specimen increased to a constant value.

Based on this framework, for the evaluation of the 3×3 multi-pixel array sensor characteristics, this study assessed the reproducibility of the pixels located in the center of the array when 20 MU was irradiated 10 times at a dose rate of 400 MU/min and an acceleration voltage of 6 MV. This accuracy and reproducibility evaluation was also performed for 5, 10, and 15 MU. The linearity evaluation was performed for each pixel for 5, 10, 15, and 20 MU under the same high-energy irradiation conditions.

We selected a material for the detection of high-energy radiation from the unit-cell-type specimens and demonstrated the feasibility of an array sensor based on the detection characteristics of each pixel of the 3×3 multi-pixel array sensor. For the 6×6 multi-pixel array sensor, to verify the dose distribution of the 1×1 mm^2 active area and the readout, we measured the dark current for one pixel and then evaluated reproducibility for 5, 10, 15 and 20 MU. Subsequently, the accuracy of 36 pixels was evaluated based on the dose values from the reproducibility results. Finally, linearity was assessed with high-energy irradiation of constantly increasing MUs.

3 Results and discussion

3.1 Physical properties of detection materials

3.1.1 Evaluation of detector characteristics

To verify the high-energy radiation conversion and detection characteristics of the four fabricated unit-cell-type specimens (PbI_2, PbO, HgI_2, and $HgI_2$and TiO_2mixture), experiments were conducted on dark current, output current, rising time, falling time, and response delay. Using an electrometer after applying -400 V to the prepared specimens, the Synergy LINAC (Elekta) was used to irradiate the specimens with X-rays at an acceleration rate of 10 MV and a dose rate of 400 MU/min. The detection characteristics of the unit-cells in this test are shown in figure 6. The HgI_2/TiO_2 mixed specimen showed the best output voltage at 4.003 V, while the PbO specimen showed the worst output voltage at 1.017×10^{-1} V. Furthermore, the HgI_2/TiO_2 mixed specimen exhibited comparatively superior high-energy radiation detection characteristics. Based on the above results, the HgI_2/TiO_2 mixed specimen was finally selected as the radiation detection material for small-field dose verification due to its superior high-energy radiation characteristics.

3.1.2 Evaluation of reactivity according to beam pulse

To perform a more accurate verification of the selected HgI_2/TiO_2 mixed unit-cell-type specimen, the conformity of the detection signals generated in the unit-cell-type specimen to the LINAC input beam pulse wave was assessed when X-rays were generated using the LINAC. We were able to confirm the signal in the detection specimen at the same time as the input pulse for the target, indicative of conformity. As shown in figure 7, the X-ray detector confirmed reactivity for the

2020 JINST 15 P04001

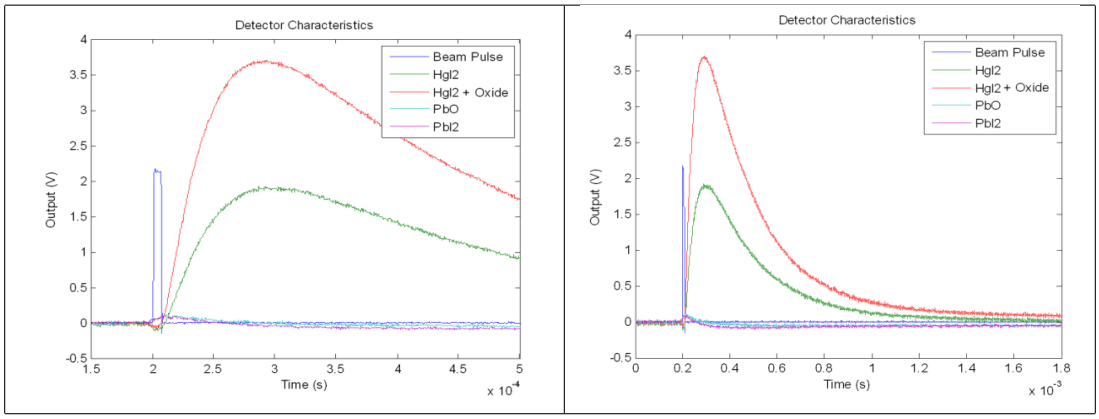

Figure 6. Characteristic graph of unit-cell-type specimens.

photons received from the radiation beam and validated the conformity between the beam pulse and the X-ray detection specimen.

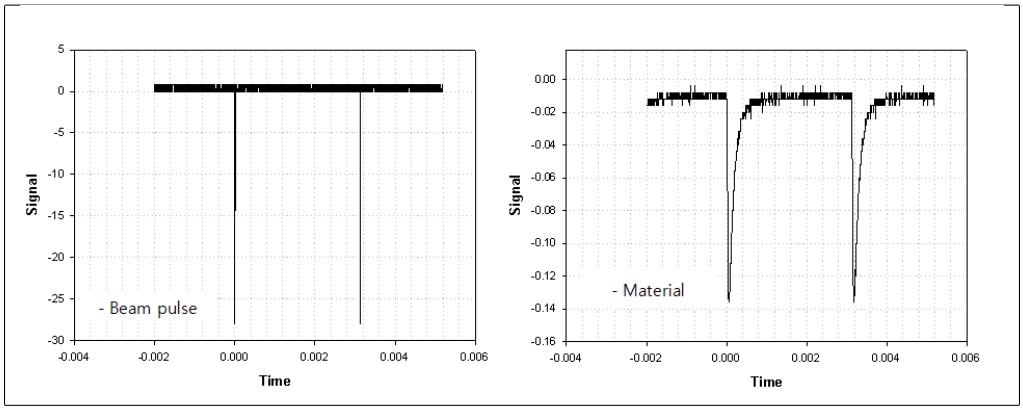

Figure 7. Signal conformity evaluation between beam pulse and radiation detection specimen for selected photoconductor material (HgI_2/TiO_2).

Reproducibility is the most important condition in radiation measurement systems from a QA perspective. This is because radiation measurement systems must always exhibit a certain reaction to the same amount of radiation to determine whether the radiation generator is generating the proper amount. Thus, a reproducibility evaluation was conducted to determine whether consistent doses were detected in the specimens during constant irradiation. For this purpose, acceleration voltages of 6 MV and 15 MV were used. All geometric conditions (SSD: 100 cm, irradiation surface size: $10 \times 10\,cm^2$, dose rate: 400 MU/min) were kept constant, and irradiation was performed 10 times at 100 MU. At 6 MV, the response of the detection specimen during 100 MU of repeated radiation provided a maximum dose of 1.83902 μC, a minimum dose of 1.8287 μC, and an average dose of 1.834429 μC, with a standard deviation of 0.0039 μC and standard error of 0.124%. At 15 MV, the specimen exhibited a maximum dose of 1.80956 μC, a minimum dose of 1.7664 μC, and an average dose of 1.78857 μC, with a standard deviation of 0.0157 μC and a standard error of 0.496%. This indicates that the fabricated unit-cell-type X-ray detector can be used in routine inspections of radiation dosing (figure 8a).

2020 JINST 15 P04001

Finally, the MU was linearly increased at the same dose rate (400 MU/min) to evaluate the linearity of the detected signal during irradiation. The unit-cell-type X-ray detection specimens were irradiated with 6 MV and 15 MV of photon energy from the LINAC at 10, 20, 30, 40, 50, 80, 100, 200, 300, 500, 800, and 1000 MU. When the MU was constantly increased at a dose rate of 400 MU/min, the detection signal of the unit-cell-type specimen exhibited a linear response to the radiation amount, as shown in figure 8b. R^2(= SSR/SST) was 1 at an acceleration voltage of 6 MV and 0.999 at 15 MV.

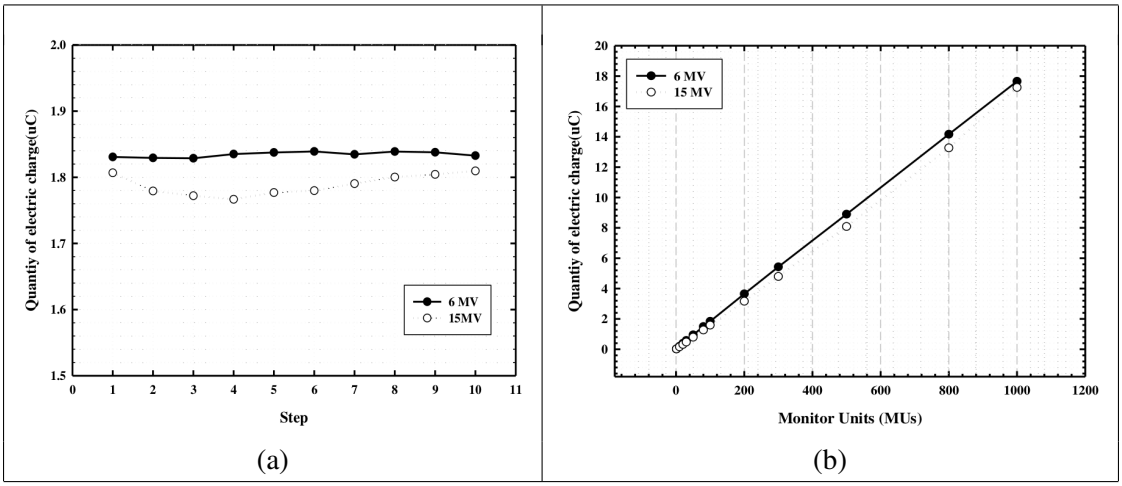

Figure 8. Evaluation of the reproducibility and linearity of selected unit-cell-type specimens: (a) reproducibility evaluation for dose detection, (b) linearity evaluation at acceleration voltages of 6 MV and 15 MV.

3.2 Multi-pixel array sensor evaluation

3.2.1 3 × 3 multi-pixel array sensor evaluation

An assessment of the reproducibility, accuracy, and linearity of a 3 × 3 multi-pixel array based on the unit-cell-type dose verification evaluation was performed. In the reproducibility evaluation, the acceleration voltage of the LINAC was fixed at 6 MV and the dose rate was fixed at 400 MU/min. Among the nine pixels, the center pixels were irradiated with 20 MU 10 times; the maximum detected dose was 1.944 μC, the minimum detected dose was 1.838 μC, the average detected dose was 1.868 μC, the standard deviation was 0.0321, and the standard error was 1.015%. The accuracy evaluation was conducted based on the average detection dose of the reproducibility evaluation. The accuracy evaluation was performed for the nine pixels with high-energy irradiation at 20 MU under the same conditions as the reproducibility evaluation. The maximum dose confirmed among the pixels was 1.944 μC, the minimum dose was 1.838 μC, and the average dose was 1.868 μC, with a standard deviation of 0.034 and a standard error of 1.13%. In addition, the accuracy evaluation was conducted with irradiation at 5, 10, 15, and 20 MU, these results are shown in figure 9a. At 5 MU, the average detected dose for the nine pixels was 0.427 μC, with a standard deviation of 0.0096 and standard error of 0.323%; at 10 MU, the average was 0.8953 μC, with a standard deviation of 0.0144 and a standard error of 0.482%; at 15 MU, this increased to an average of 1.4896 μC, with a standard deviation of 0.0239 and a standard error of 0.797%.

2020 JINST 15 P04001

In the linearity evaluation, it was determined that the detected dose increased linearly at a constant irradiation of 5, 10, 15, or 20 MU, a fixed dose rate of 400 MU/min and an acceleration voltage of 6 MV for all pixels. As shown in figure 9b, the R^2 values of channels 1–9 (each pixel) were 0.995, 0.9939, 0.9933, 0.9931, 0.9936, 0.9934, 0.9936, 0.993, and 0.9927, respectively, demonstrating strong linearity.

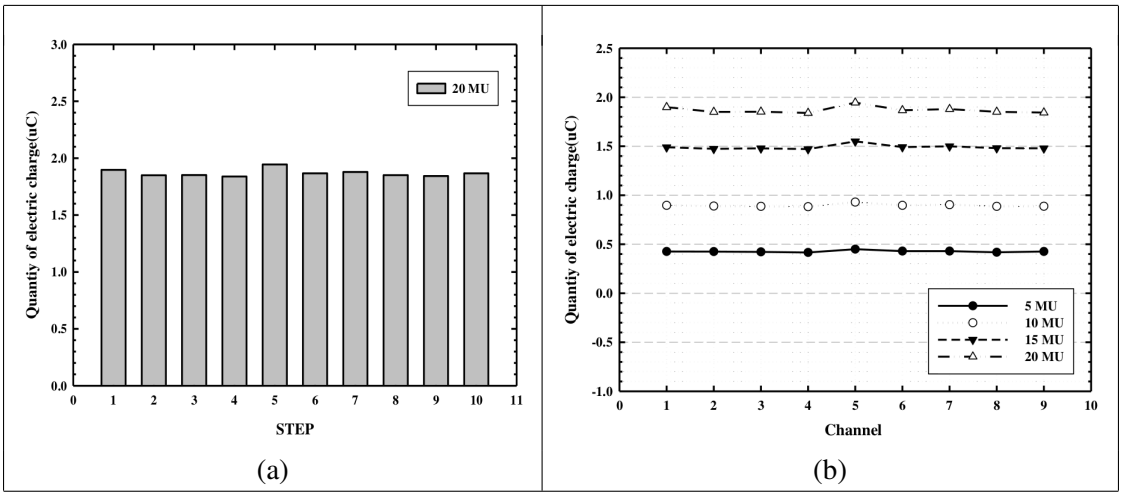

Figure 9. (a) Accuracy and (b) reproducibility evaluation of 3 × 3 multi-pixel array sensors.

3.2.2 6 × 6 multi-pixel array sensor evaluation

As shown in figure 10, a sensor with 36 pixels each with a diameter of 1 mm was fabricated in order to perform small-field dose verification during medical high-energy irradiation from a LINAC. Before evaluating the reproducibility, accuracy, and linearity of each pixel, +490 V and -490 V were applied to the 6 × 6 multi-pixel array sensor using an electrometer in a dark room at 2 min intervals for a total time of 20 min and the dark current was measured. At -490 V, a maximum dark current of 3.79 nC — excluding the current of 41.540 nC measured at initial voltage application—and a minimum current of 3.47 nC were recorded. The average was 3.665 nC. In addition, at +490 V, a maximum dark current of 4.95 nC and a minimum dark current of 3.82 nC were recorded, with an average of 4.332 nC.

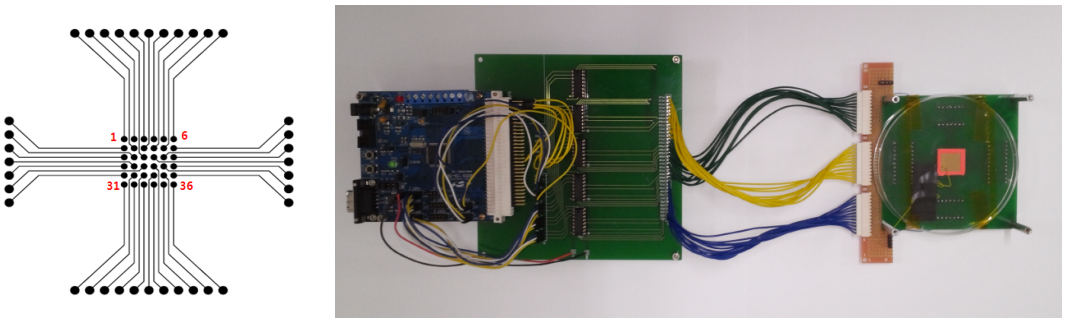

Figure 10. Fabricated 6 × 6 multi-pixel array sensor.

2020 JINST 15 P04001

For the reproducibility evaluation, high-energy irradiation of 100 MU was repeatedly delivered at a dose rate of 400 MU/min; figure 11b shows the doses of the center pixel. A maximum dose of 1.1426 µC, a minimum dose of 1.0365 µC, an average dose of 1.0682 µC, a standard deviation of 0.0356, and a standard error of 1.127% were recorded. For the accuracy evaluation — using the reproducibility values obtained from 10 repeated irradiations of one pixel — the 36 pixels were irradiated at a dose rate of 400 MU/min at 100 MU and an acceleration voltage of 6 MV. This test evaluated whether the dose detected in each pixel was the same. Figure 11c shows the dosimetry results. At 100 MU, the average detected dose for the 36 pixels was 1.069972 µC, with a standard deviation of 0.0407 and a standard error of 0.679%.

For the linearity evaluation of the 6 × 6 multi-pixel array sensor, the nine pixels were irradiated with 10, 20, 50, 100, and 200 MU with a fixed acceleration of 6 MV and a dose rate of 400 MU/min. Figure 11d shows the detected doses for certain MUs. The R^2 values of channels 1, 6, 8, 11, 16, 26, 29, 31, and 36 were 0.9997, 0.9997, 0.9991, 0.9995, 0.9995, 0.9992, 0.9996, 0.9997, and 0.9995, respectively, demonstrating strong linearity.

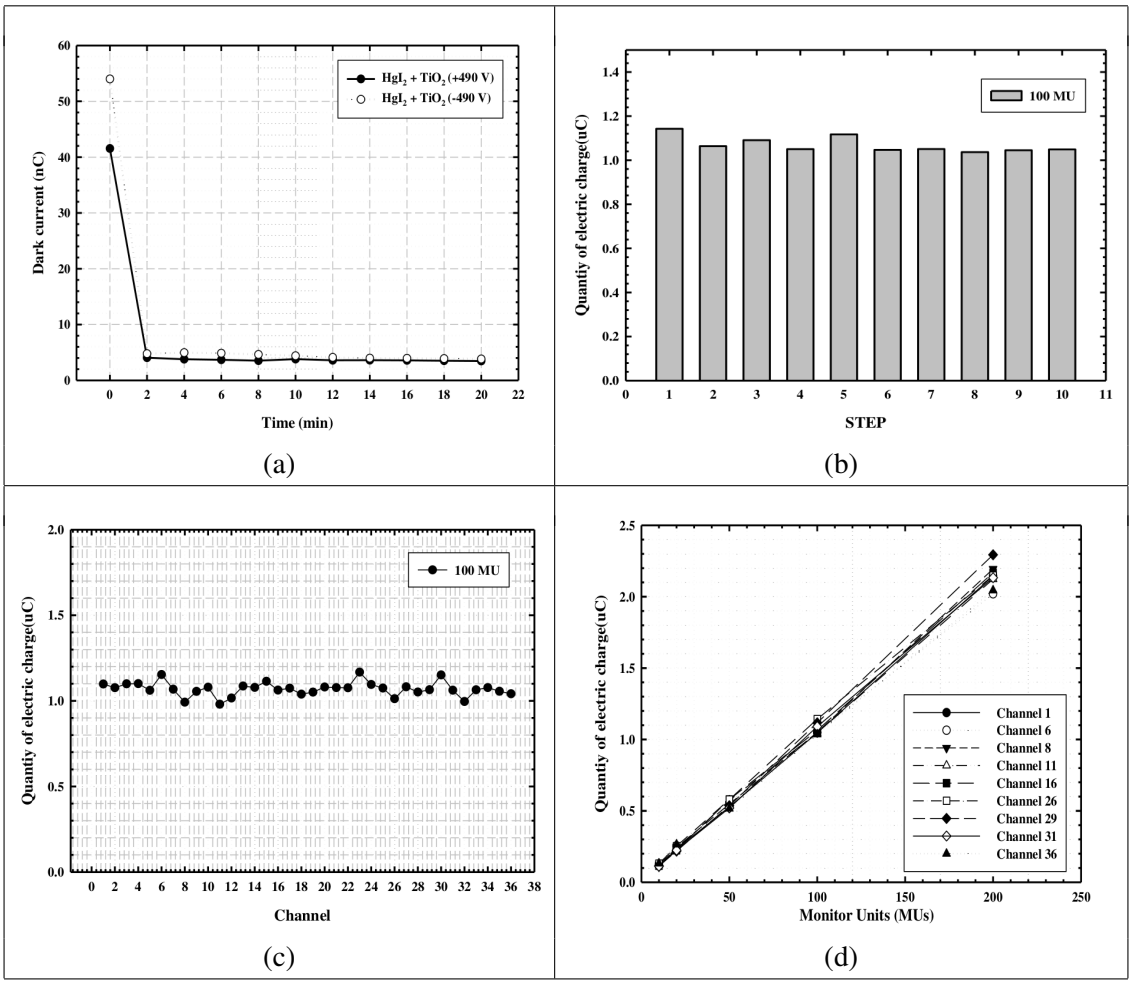

Figure 11. Evaluation of (a) dark current, (b) reproducibility, (c) accuracy, and (d) linearity for a 6 × 6 multi-pixel array sensor.

2020 JINST 15 P04001

4 Conclusion

This study performed high-energy X-ray small-field QA and dose verification for a medical LINAC. For this purpose, the detection characteristics of photoconductor materials that are being researched for radiation detection were analyzed. A mixture of HgI_2 and TiO_2 was selected as an optimal photoconductor for small-field dose verification. Using this material, we confirmed the same signal amplitude for the beam pulse waveform of the LINAC and the detection signal for approximately 0.0032 s. In the reproducibility evaluation, at an acceleration voltage of 15 MV, the specimen was irradiated 10 times at 100 MU and exhibited a maximum dose of 1.80956 μC, a minimum dose of 1.7664 μC, and an average dose of 1.78857 μC, with a standard deviation of 0.0157 μC and standard error of 0.496%, demonstrating excellent reproducibility. Furthermore, the detected dose measured during the linearity evaluation was within an error range of 1%, further indicating conformity. This suggests that the selected radiation detection material is sufficient for use in routine inspections of the medical LINAC for high-energy radiation. On this basis, the reproducibility, accuracy, and linearity of a multi-pixel array sensor based on the fabricated high-energy radiation dose detector using HgI_2/TiO_2 were evaluated. The 3×3 multi-pixel array sensor exhibited a standard error of 1.015%, and a minimum standard error of 0.323% for accuracy. The linearity evaluation also showed excellent linearity with R^2 values close to 1. Based on these results, we fabricated a 6×6 multi-pixel array sensor with diameters of 1 mm, which facilitates small-field dose verification. The evaluation of this sensor showed reproducibility with a standard error of 1.127%. In terms of accuracy, the average detection dose was 1.069 μC with a standard deviation of 0.0407 and a standard error of 0.769%. As the pixel size decreased, the standard error increased slightly in the reproducibility evaluation compared to the 3×3 multi-pixel array sensor due to the influence of pixel interference around the target. However, the 6×6 array sensor had better linearity than the 3×3 sensor. This evaluation measures the detection of high-energy radiation with regards to accuracy during constant increases in MUs. In particular, the standard error of 0.323% obtained in the accuracy evaluation is superior to the error rate of 0.4–1% observed in current commercialized thermoluminescence dosimeters, diode detectors, ionization chambers, diamond detectors, and films that verify high-energy radiation doses utilized in stereotactic radiosurgery. Furthermore, previous literature suggests that the mixture of TiO_2 and HgI_2 is very responsive to radiation, even in light conditions. This indicates that the QA tasks could be performed more quickly, conveniently, and economically by using a single device for both radiation and light detection. Thus, this study presented the feasibility of a QA device that facilitates dosimetry for small-field irradiation from medical LINACs.

Acknowledgments

This research was supported by the Dongnam Institute of Radiological & Medical Sciences (DIRAMS) grant funded by the government of Korea (MIST) [grant number 50496-2020].

References

[1] A. McNiven, T. Kron and J. Van Dyk, *A multileaf collimator phantom for the quality assurance of radiation therapy planning system and CT simulators*, *Int. J. Radiat. Oncol. Biol. Phys.* **60** (2004) 994.

2020 JINST 15 P04001

[2] S. Bujenovic, *The role of positron emission tomography in radiation treatment planning*, *Semin. Nucl. Med.* **34** (2004) 293.

[3] International Commission on Radiological Units (ICRU), *Determination of absorbed dose in patient irradiated by beams of X and gamma rays in radiotherapy procedures*, ICRU Report 24 (1976).

[4] International Commission on Radiological Units (ICRU), 1978 *Dose specification for reporting external beam therapy with photons and electrons*, ICRU Report 29 (1978).

[5] International Commission on Radiological Units (ICRU), 1985 *Dose and volume specification for reporting intracavitary therapy in gynaecology*, ICRU Report 38 (1985).

[6] International Commission on Radiological Units (ICRU), 1987 *Use of computers in external beam radiotherapy procedure with high-energy photons and electrons*, ICRU Report 42 (1987).

[7] International Commission on Radiological Units (ICRU), 1992 *Phantoms and computational models in therapy, diagnosis and protection*, ICRU Report 48 (1992).

[8] International Commission on Radiological Units (ICRU), *Prescribing, recording and reporting photon beam therapy*, ICRU Report 50 (1993).

[9] Nordic Association of Clinical Physics (NACP), *Procedures in external radiation therapy: Dosimetry with electron and photons beams with maximum energy between 1 and 50 MeV*, *Acta Radiol. Oncol.* **19** (1980) 55.

[10] A.F. Monti, M. Frigerio and G. Frigerio, *Visual verification of LINAC light and radiation fields coincidence*, *Med. Dosim.* **28** (2003) 91.

[11] P. Dumscombe, S. Humphreys and K. Leszczynsky, *A test tool for the visual verification of light and radiation fields using film or an electronic portal imaging device*, *Med. Phys.* **26** (1999) 239.

[12] B.R. Tomadsen, A.K. Ho and S. Shahabi, *The use of Polaroid TPX radiographic film for light localization-radiation fields coincidence testing*, *Phys. Med. Biol.* **35** (1990) 115.

[13] T. LoSasso, C. Chui and C. Ling, *Physical and dosimetric aspects of a multileaf collimation system used in the dynamic mode for implementing intensity modulation radiotherapy*, *Med. Phys.* **25** (1998) 1919.

[14] A.T. Lintereur, Q. Wei, J.C. Nino and J.E. Baciak, *Iodine based compound semiconductors for room temperature gamma-ray spectroscopy*, *Proc. SPIE* **3945** (2008) 694503.

[15] S.O. Kasap, *Photoreceptors: The selenium alloys*, in *The Handbook of Imaging Materials*, Marcel Dekker, New York U.S.A. (1991), pg. 329.

[16] J.M. Boone, J.A. Seibert, J.M. Sabol and M. Tecotzky, *A Monte Carlo study of X-ray fluorescence in X-ray detectors*, *Med. Phys.* **26** (1999) 905.

[17] A. Tsukamoto et al., *Development of a selenium based flat-panel detector for real-time radiography and fluoroscopy*, *Proc. SPIE* **3336** (1998) 388.

[18] E.J. Harold and J.R. Cunningham, *The physics of radiology*, fourth edition, Thomas Books, Toronto Canada (1983).

[19] J.T. Bushberg, J.M. Boone and J.A. Seibert, *The essential physics of Medical imaging*, second edition, Wolters Kluwer Company, Sacramento U.S.A. (2000).

[20] H.B. Richard, *Photoconductivity of solids*, second edition, John Wiley & Sons, New York U.S.A. (1967).

[21] K.M. Oh et al., *Flexible X-ray detector for automatic exposure control in digital radiography*, *J. Nanosci. Nanotechnol.* **16** (2016) 11473.

2020 JINST 15 P04001